Available online at www.sciencedirect.com
ScienceDirect
Polyhedron 26 (2007) 851–861
POLYHEDRON
www.elsevier.com/locate/poly

# Palladium complexes of multidentate pyrazolylmethyl pyridine ligands: Synthesis, structures and phenylacetylene polymerization

Stephen O. Ojwach [a], Ilia A. Guzei [b], James Darkwa [a,*], Selwyn F. Mapolie [c]

[a] Department of Chemistry, University of Johannesburg, Auckland Park Kingsway Campus, Auckland Park 2006, South Africa
[b] Department of Chemistry, University of Wisconsin-Madison, 1101 University Avenue, Madison, WI 53706, USA
[c] Department of Chemistry, University of the Western Cape, Private Bag X17, Bellville 7535, South Africa

Received 7 August 2006; accepted 14 September 2006
Available online 22 September 2006

**Abstract**

The compounds, 2,6-bis(3,5-dimethylpyrazol-1-ylmethyl)pyridine ($_{Me}$NNN) (**L1**) and 2,6-bis(3,5-ditertbutylpyrazol-1-ylmethyl)pyridine ($_{tBu}$NNN) (**L2**), react with either $[Pd(NCMe)_2Cl_2]$ or [Pd(COD)ClMe] to form the mononuclear palladium complexes $[Pd(_{Me}NNN)Cl_2]$ (**1**), [Pd($_{Me}$NNN)ClMe] (**2**), $[Pd(_{tBu}NNN)Cl_2]$ (**3**) and [Pd($_{tBu}$NNN)ClMe] (**4**). Reactions of **1**, **2** and **4** with the halide abstractor, $NaBAr_4$ (Ar = 3,5-$(CF_3)_2C_6H_3$), led to the formation of stable tridentate cationic species $[Pd(_{Me}NNN)Cl]^+$(**5**), $[Pd(_{Me}NNN)Me]^+$ (**6**) and $[Pd(_{tBu}NNN)Cl]^+$ (**7**) respectively. The analogous carbonyl linker cationic species $[Pd\{(3,5\text{-}Me_2pz\text{-}CO)_2\text{-}py\}Cl]^+$ (**9**) and $[Pd\{(3,5\text{-}^tBu_2pz\text{-}CO)_2\text{-}py\}Cl]^+$ (**10**), prepared by halide abstraction of the neutral complexes $[Pd\{(3,5\text{-}Me_2pz\text{-}CO)_2\text{-}py\}Cl_2]$ and $[Pd\{(3,5\text{-}^tBu_2pz\text{-}CO)_2\text{-}py\}Cl_2]$ by $NaBAr_4$, were however less stable with $t_{1/2}$ of 14 and 2 days respectively. Attempts to crystallize **1** and **3** from the mother liquor resulted in the isolation of the salts $[Pd(_{Me}NNN)Cl]_2[Pd_2Cl_6]$ (**11**) and $[Pd(_{tBu}NNN)Cl]_2[Pd_2Cl_6]$ (**12**). Although when complexes **1**–**4** were reacted with modified methylaluminoxane (MMAO) or $NaBAr_4$, no active catalysts for ethylene oligomerization or polymerization were formed, activation with silver triflate (AgOTf) produced active catalysts that oligomerized and polymerized phenylacetylene to a mixture of *cis-transoidal* and *trans-cisoidal* polyphenylacetylene.


*Keywords:* (Pyrazolylmethyl)pyridine; Bidentate palladium complexes; Tridentate ligand coordination; Cationic palladium complexes; Phenylacetylene; Polymerization

## 1. Introduction

Multidentate nitrogen based ligands, such as 2,6-bis(organylimino)pyridine and 2,6-bis(pyrazol-1-ylmethyl)-pyridine late transition metal complexes, are good catalysts for the oligomerization and polymerization of olefins [1]. Other nitrogen based ligands such as bidentate α-diimine are also known to form cationic Ni and Pd complexes that polymerize or oligomerize olefins depending on the steric bulk of the ligand backbone [2]. These cationic α-diimine Ni and Pd complexes are often prepared by direct halide abstraction using silver or alkali metal salts of a very weakly coordinating or non-coordinating counter ion. It has been established that the presence of strongly coordinating ligands compete with the monomer for the vacant coordination site in the active catalyst [3]. It is therefore essential to have a weakly coordinating ligand that would not compete with the incoming monomer for the vacant site of the metal and yet would protect the metal in the absence of the substrate.

Recently we have used 2,6-bis(pyrazol-1-ylcarbonyl)pyridine palladium dichloride complexes as catalyst precursors for ethylene polymerization [4]. The ligands in these precursors are potentially tridentate but only coordinate in a bidentate mode through one pyrazolyl and the pyridine nitrogen atoms leaving the second pyrazolyl unit uncoordinated.

* Corresponding author. Tel.: +27 11 489 2838; fax: +27 11 489 2819.
*E-mail address:* jdarkwa@uj.ac.za (J. Darkwa).

0277-5387/$ - see front matter © 2006 Elsevier Ltd. All rights reserved.
doi:10.1016/j.poly.2006.09.007

When the complexes are reacted with methylaluminoxane (MAO) as co-catalysts, they form active catalysts for the polymerization of ethylene to give high density polyethylene (HDPE) [4]. However, the expected activity in comparison with our previous catalysts generated from 1,3-bis(pyrazol-1-yl)benzene [5a] is considerably lower, possibly due to the potential of 2,6-bis(pyrazol-1-ylcarbonyl)pyridine to bind in a tridentate coordination mode upon removal of a chloride (Scheme 1). This is likely to result in the ethylene monomer competing with the second pyrazolyl unit in coordinating to the vacant site on the metal in the catalyst (Scheme 1, route B).

The stability of the carbonyl linker catalysts was also found to be lower than the bis(pyrazole)palladium(II) catalysts [5b] and in an attempt to produce more stable catalysts we have replaced the carbonyl linker with a methylene group. Some of the chemistry of 2,6-bis(pyrazol-1-ylmethyl)pyridine have earlier been explored by Steel et al. [6] and others [7]. In a report by Steel et al. [6a] a palladium dichloride complex with this ligand system was formulated as a trinuclear complex with three ligand units. We found 2,6-bis(pyrazol-1-ylmethyl)pyridine to complex with palladium dichloride fragments in a bidentate fashion; bonding through one pyrazolyl nitrogen and the pyridine nitrogen, with the second pyrazolyl unit uncoordinated. The latter coordinates to the palladium metal upon chloride abstraction. These findings and attempts to use the palladium complexes as ethylene and phenylacetylene polymerization catalysts are described in this paper.

## 2. Experimental

### 2.1. Materials and instrumentation

Synthetic and $^1$H NMR experimental manipulations were performed under a nitrogen atmosphere using standard Schlenk techniques and glove box. All solvents were of analytical grade and were dried and distilled prior to use. Toluene and dichloromethane were dried and distilled from sodium/benzophenone and $P_2O_5$ respectively.

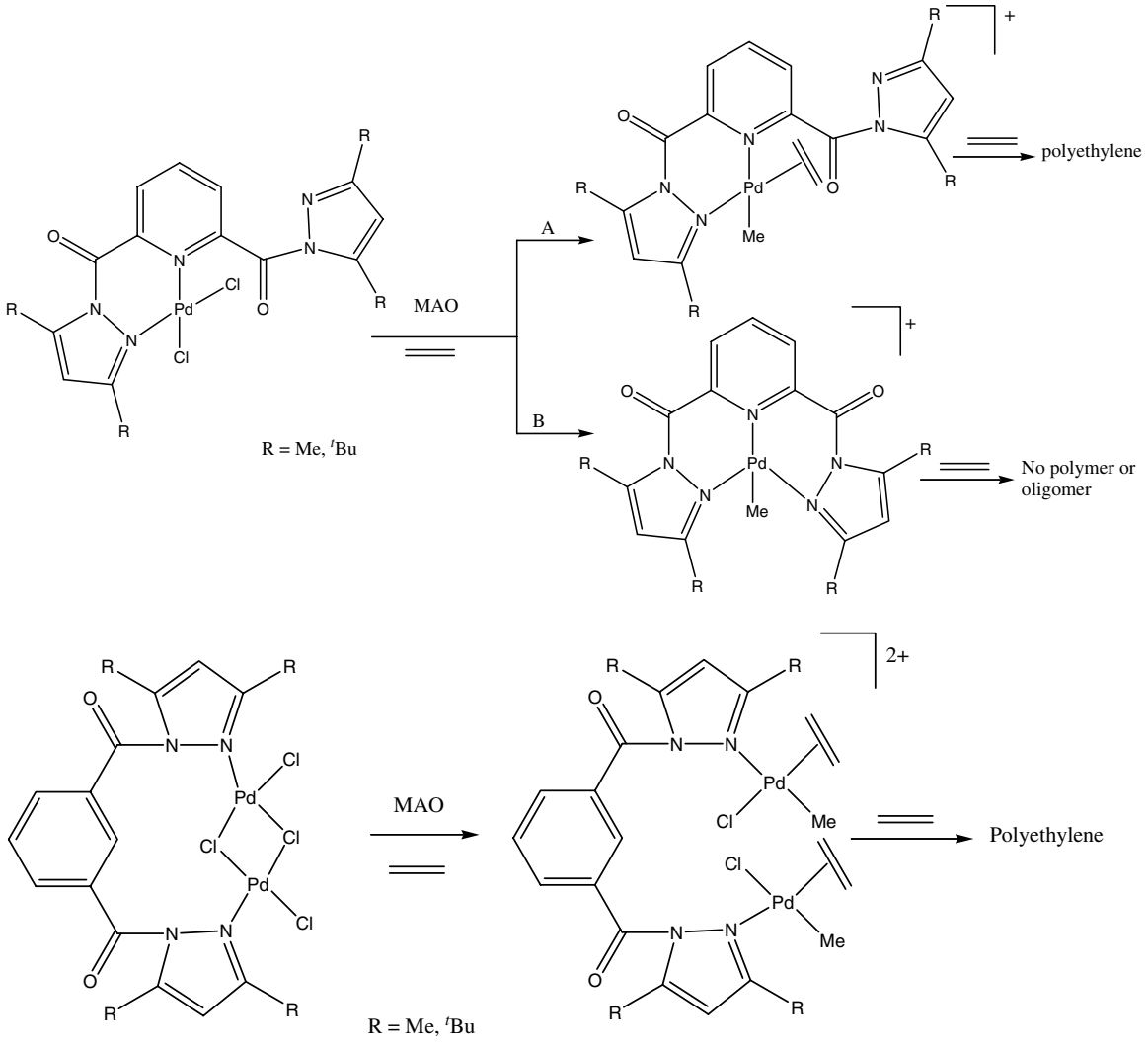


Scheme 1.

2,6-Bis(chloromethyl)pyridine, tetrabutylammonium bromide, silver triflate and phenylacetylene (98%) were obtained from Sigma–Aldrich and used as received. $NaBAr_4$ ($Ar = 3,5\text{-}(CF_3)_2C_6H_3$) was obtained from Boulder Scientific and used as received. The starting materials 3,5-ditertbutylpyrazole [8], [Pd(COD)MeCl] [9,10] and 2,6-bis(3,5-dim-ethylpyrazol-1-ylmethyl)pyridine (**L1**) [6a] were synthesized following the literature procedures. The NMR spectra were recorded on a Varian Gemini 2000 instrument ($^1H$ at 200 MHz and $^{13}C$ at 50.1 MHz) at room temperature. The chemical shifts are reported in $\delta$ (ppm) and referenced to the residual $CHCl_3$ in the NMR solvent. Coupling constants are measured in Hertz (Hz). Elemental analyses were performed by the micro analytical laboratory at the University of Cape Town, South Africa, as a service. Polymer molecular weights were determined by gel permeation chromatography on a Waters 600E instrument equipped with a Waters differential refractometer detector (THF, at 30 °C, rate = 1.0 mL/min) and PL–MIXED-C…™ columns, using polystyrene standards.

### 2.2. Synthesis of ligands and palladium complexes

#### 2.2.1. 2,6-{(3,5-$^t$Bu$_2$pzCH$_2$)$_2$py} (*L2*)

A mixture of 2,6-bis(bromomethyl)pyridine (1.00 g, 3.79 mmol) and 3,5-di-*tert*-butylpyrazole (1.36 g, 7.58 mmol) in benzene (40 mL), 40% aqueous NaOH (12 mL) and 40% aqueous tetrabutylammonium bromide (10 drops) was refluxed for 18 h. The organic layer was then separated, and evaporated *in vacuo*. The crude product was washed with water (40 mL) to afford an analytically pure compound **L2** as a white solid. Yield = 1.38 g (75%). $^1H$ NMR ($CDCl_3$): $\delta$ 1.23 (18H, s, $^t$Bu, pz); 1.31 (18H, s, $^t$Bu, pz); 5.55 (4H, s, $CH_2$); 5.93 (2H, s, 4H-pz); 6.32 (2H, d, 3,5H-py, $^3J_{HH} = 8.0$); 7.46 (1H, t, 4H-py, $^3J_{HH} = 8.0$). *Anal.* Calc. for $C_{29}H_{45}N_5$: C, 75.16; H, 9.72; N, 15.12. Found: C, 75.01; H, 9.55; N, 15.43%.

#### 2.2.2. [Pd($_{Me}$ÑÑN)Cl$_2$] (*1*)

To a solution of **L1** (0.11 g, 0.39 mmol) in $CH_2Cl_2$ (20 mL) was added $[Pd(NCMe)_2Cl_2]$ (0.10 g, 0.39 mmol). The pink solution was stirred for 12 h and the product precipitated by addition of hexane (20 mL) to give a pink solid. Yield = 0.10 g (56%). $^1H$ NMR ($CDCl_3$): $\delta$ 2.45 (6H, s, $CH_3$, pz); 2.51 (6H, s, $CH_3$, pz); 5.85 (2H, d, $CH_2$, $^2J_{HH} = 15.2$); 5.93 (1H, s, 4H-pz); 6.17 (2H, d, $CH_2$, $^2J_{HH} = 15.0$); 6.28 (1H, s, 4H-pz); 8.11 (2H, d, 3,5H-py, $^3J_{HH} = 8.4$); 8.26 (1H, t, 4H-py, $^3J_{HH} = 8.4$). *Anal.* Calc. for $C_{17}H_{21}N_5PdCl_2$: C, 43.22; H, 4.44; N, 14.83. Found: C, 43.31; H, 4.10; N, 14.91%.

#### 2.2.3. [Pd($_{Me}$ÑÑN)MeCl] (*2*)

To a solution of **L1** (0.30 g, 1.07 mmol) in $Et_2O$ (20 mL) was added a solution [Pd(COD)ClMe] (0.27 g, 1.07 mmol) in $Et_2O$ (20 mL). A light yellow precipitate was formed immediately. The mixture was stirred for 3 h, filtered and the material isolated recrystallized from $CH_2Cl_2$–hexane to give a light yellow solid. Yield = 0.31 g (68%). $^1H$ NMR ($CDCl_3$): $\delta$ 0.97 (3H, s, $CH_3$,Pd–Me); 2.34 (6H, s, $CH_3$, pz); 2.49 (6H, s, $CH_3$, pz); 5.68 (2H, d, $CH_2$, $^2J_{HH} = 15.4$); 5.74 (d, 2H, $CH_2$, $^2J_{HH} = 15.4$); 5.91 (2H, s, 4H-pz); 8.08 (1H, t, 4H-py, $^3J_{HH} = 8.4$); 8.15 (2H, d, 3,5H-py, $^3J_{HH} = 8.2$). $^{13}C$ NMR ($CDCl_3$): $\delta$ −7.4; 12.3; 14.9; 52.6; 108.2; 125.3; 141.7; 143.2; 151.8; 152.0. *Anal.* Calc. for $C_{18}H_{24}N_5PdCl \cdot CH_2Cl_2$: C, 42.53; H, 4.85; N, 13.06. Found: C, 42.31; H, 4.77; N, 11.64%.

#### 2.2.4. [Pd($_{tBu}$ÑÑN)Cl$_2$] (*3*)

To a solution of $[Pd(NCMe)Cl_2]$ (0.20 g, 0.78 mmol) in $CH_2Cl_2$ (20 mL) was added **L2** (0.36 g, 0.78 mmol). The clear orange solution was stirred for 24 h after which an equal volume of hexane was added and kept at −4 °C to afford compound **3** as a yellow solid. Single crystals suitable for X-ray analysis were obtained by slow evaporation of $CDCl_3$ used as $^1H$ NMR solvent. Yield = 0.35 g (71%). $^1H$ NMR ($CDCl_3$): $\delta$ 1.27 (9H, s, $^t$Bu, pz); 1.34 (9H, s, $^t$Bu, pz); 1.41 (9H, s, $^t$Bu, pz); 1.75 (9H, s, $^t$Bu, pz); 5.72 (1H, d, $CH_2$, $^2J_{HH} = 18.6$); 5.78 (1H, d, $CH_2$, $^2J_{HH} = 15.4$); 5.92 (1H, s, 4H-pz); 5.97 (1H, s, 4H-pz); 6.23 (1H, d, $CH_2$, $^2J_{HH} = 15.6$); 7.01 (1H, d, $CH_2$, $^2J_{HH} = 19.0$); 7.44 (2H, d, 3,5H-py, $^3J_{HH} = 8.0$); 7.69 (1H, t, 4H-py, $^3J_{HH} = 8.0$). $^{13}C$ NMR ($CDCl_3$): $\delta$ 30.1; 30.2; 30.6; 31.1; 31.4; 31.8; 32.0; 33.0; 56.4; 56.7; 100.8; 104.3; 122.9; 124.0; 140.4; 153.2; 154.0; 155.2; 162.0; 164.3; 164.6. *Anal.* Calc. for $C_{29}H_{45}N_5PdCl_2 \cdot 0.5CH_2Cl_2$: C, 52.33; H, 6.59; N, 10.17. Found: C, 52.72; H, 7.08; N, 10.26%.

#### 2.2.5. [Pd($_{tBu}$ÑÑN)MeCl] (*4*)

Compound **4** was prepared according to the procedure for **2** using **L2** (0.21 g, 0.45 mmol) and [Pd(COD)MeCl] (0.12 g, 0.45 mmol). Yield = 0.17 g (60%). $^1H$ NMR ($CDCl_3$): $\delta$ 1.03 (3H, s, $CH_3$, Pd–Me); 1.23 (9H, s, $^t$Bu, pz); 1.35 (9H, s, $^t$Bu, pz); 1.41 (9H, s, $^t$Bu, pz); 1.61 (9H, s, $^t$Bu, pz); 5.35 (1H, d, $CH_2$, $^2J_{HH} = 18.6$); 5.53 (1H, d, $CH_2$, $^2J_{HH} = 15.0$); 5.93 (1H, s, 4H-pz); 5.95 (1H, s, 4H-pz); 6.11 (1H, d, $CH_2{}^2J_{HH} = 15.4$); 6.87 (1H, d, $CH_2$, $^2J_{HH} = 19.2$); 7. 21 (2H, d, 3,5H-py, $^3J_{HH} = 8.0$); 7.69 (1H, t, 4H-py, $^3J_{HH} = 8.0$). $^{13}C$ NMR ($CDCl_3$): $\delta$ 30.1; 30.4; 30.6; 31.1; 31.5; 32.6; 55.7; 100.3; 103.8; 121.8; 122.2; 138.5; 152.8; 153.7; 162.1. *Anal.* Calc. for $C_{30}H_{48}N_5PdCl$: C, 58.06; H, 7.80; N, 11.28. Found: C, 58.10; H, 8.32; N, 10.13%.

The synthesis of **6** and **7** are described as examples of how the cationic complexes were prepared.

#### 2.2.6. [Pd($_{Me}$ÑÑN)Me]BAr$_4$ (*6*)

To a solution of **2** (0.05 g, 0.11 mmol) in $CH_2Cl_2$ (10 mL) was added a solution of $NaBAr_4$ (0.10 g, 0.11 mmol) in $CH_2Cl_2$ (10 mL) and stirred for 10 min. The resultant mixture containing Pd black was filtered over Celite to give a clear solution. Hexane (20 mL) was added to the filtrate and kept at −4 °C to afford colourless single crystals suitable for X-ray analysis. Yield = 0.15 g (30%). $^1H$ NMR ($CDCl_3$): $\delta$ 1.09 (s, 3H, $CH_3$, Pd–Me); 2.30

(6H, s, $CH_3$, pz); 2.35 (6H, s, $CH_3$, pz); 5.14 (2H, d, $CH_2$, $^2J_{HH} = 15.0$); 5.70 (2H, d, $CH_2$, $^2J_{HH} = 15.0$); 5.95 (2H, s, 4H-pz); 7.22 (2H, d, 3,5H-py, $^3J_{HH} = 8.0$). 7.55 (1H, t, 4H-py, $^3J_{HH} = 8.2$); 7.49 (4H, s, $H_p$, $BAr_4$); 7.68 (8H, s, $H_o$, $BAr_4$). *Anal.* Calc. for $C_{50}H_{36}BF_{24}N_5Pd$: C, 46.92; H, 2.73; N, 5.47. Found: C, 47.45; H, 2.48; N, 5.48%.

### 2.2.7. $[(_{tBu}\hat{N}\hat{N}N)PdCl]BAr_4$ (7)

This compound was synthesized according to the procedure described for **6** using **3** (0.09 g, 0.13 mmol) and $NaBAr_4$ (0.12 g, 0.13 mmol) which gave **7** as a crystalline orange solid. Yield = 0.11 g (58%). $^1$H NMR ($CDCl_3$): $\delta$ 1.43 (18H, s, $^t$Bu, pz); 1.52 (18H, s, $^t$Bu, pz); 5.68 (2H, d, $CH_2$, $^2J_{HH} = 15.2$); 6.08 (2H, s, 4H-pz); 6.21 (2H, d, $CH_2$, $^2J_{HH} = 15.2$); 7.27 (2H, d, 3,5H-py, $^3J_{HH} = 8.0$); 7.50 (1H, t, 4H-py, $^3J_{HH} = 8.0$); 7.49 (4H, s, $H_p$, $BAr_4$); 7.68 (8H, s, $H_o$, $BAr_4$). *Anal.* Calc. for $C_{59}H_{57}BF_{24}N_5PdCl$: C, 49.05; H, 3.98; N, 4.85. Found: C, 49.51; H, 4.00; N, 4.97%.

## 2.3. Phenylacetylene oligomerization and polymerization

In a typical experiment, a solution of AgOTf (0.05 g, 0.2 mmol) in a 20 mL mixture of $CH_2Cl_2$ and MeCN (1:1) was added to a complex solution of **1** (0.05 g, 0.1 mmol) in $CH_2Cl_2$ (20 mL). A white precipitate of AgCl formed immediately, the mixture was stirred for 5 min and filtered to give a yellow solution of the active catalyst. To this solution was added 50 equiv. of phenylacetylene monomer (0.64 mL, 5 mmol). The yellow solution gradually turned dark red and was stirred for a further 1 h. After the reaction period, the solution was evaporated to dryness to afford a dark brown crude product, which was dissolved in minimum amount of $CH_2Cl_2$ and the polymer precipitated from methanol (40 mL). This was dried and weighed to obtain the percent polymer. The methanol solution was allowed to evaporate to dryness to obtain the oligomer fractions. Both the oligomers and polymers were characterized by of $^1$H NMR spectroscopy and gel permeation chromatography.

## 2.4. X-ray crystallography

Crystal evaluation and data collection for **3**, **5**, **6**, **11** and **12** were performed on a Bruker CCD-1000 diffractometer with Mo K$\alpha$ ($\lambda = 0.71073$ Å) radiation and the diffractometer to crystal distance of 4.9 cm. The initial cell constants were obtained from three series of $\omega$ scans at different starting angles. The reflections were successfully indexed by an automated indexing routine built in the SMART program. The absorption correction was based on fitting a function to the empirical transmission surface as sampled by multiple equivalent measurements [11]. The structures were solved by direct methods and refined by least-squares techniques using SHELXTL program [11]. All non-hydrogen atoms were refined with anisotropic displacement coefficients. All hydrogen atoms were included in the structure factor calculation at idealized positions and were allowed to ride on the neighbouring atoms with relative isotropic displacement coefficients.

## 3. Results and discussion

## 3.1. Synthesis of bis(pyrazol-1-ylmethyl)pyridine palladium complexes

Compound 2,6-bis(3,5-ditertbutylpyrazol-1-ylmethyl)-pyridine ($_{tBu}\hat{N}\hat{N}N$) (**L2**) was prepared in good yields (75%) via phase transfer catalyzed alkylation of 3,5-ditertbutylpyrazole and 2,6-bis(bromomethyl)pyridine following the literature procedure [6a] described for the synthesis of 2,6-bis(3,5-dimethylpyrazol-1-ylmethyl)pyridine ($_{Me}\hat{N}\hat{N}N$) (**L1**). Compounds **L1** and **L2** reacted with either $[Pd(NCMe)_2Cl_2]$or [Pd(COD)ClMe] to produce the corresponding complexes **1**–**4** in moderate to good yields (Scheme 2).

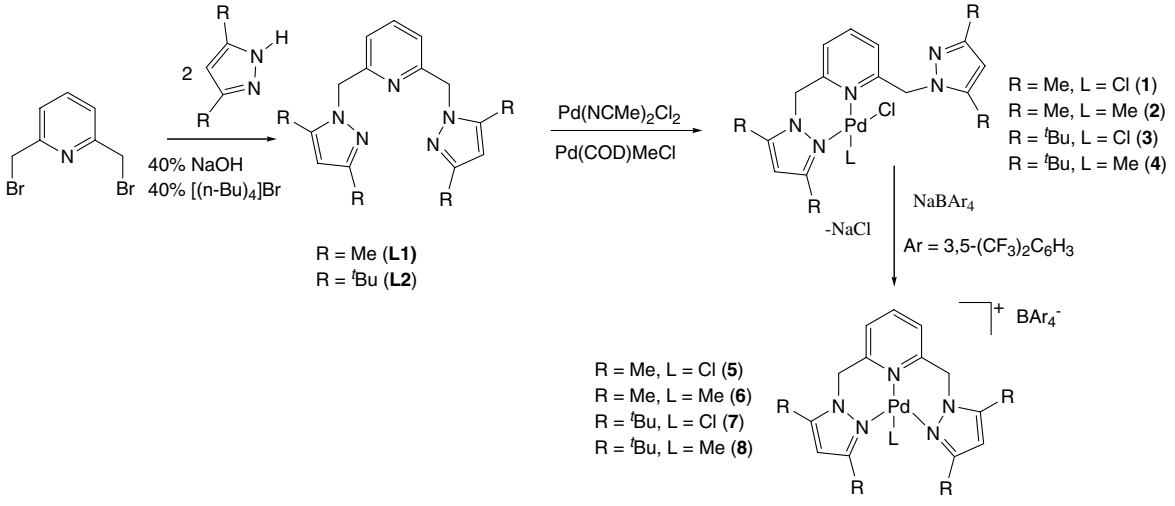


Scheme 2.

The $^1$H NMR spectra of **L1** and **L2** gave signature peaks of the four $CH_2$ linker protons as singlets at 5.28 and 5.55 ppm respectively and typical peaks of methyl and tertbutyl at 2.25 and 2.51 ppm and 1.21 and 1.31 ppm respectively. These peaks were diagnostic in the next step to confirm that complexation of the ligands with the palladium salts had occurred. On complexation of **L1** and **L2**, the $CH_2$ linker protons appeared as AB quartets. In complexes **1** and **2** these signals are between 5.68–6.17 ppm (**L1** singlet, 5.28 ppm) confirming the presence of diastereotopic protons in axial and equatorial positions. This inequality arises from different chair and boat conformations that depict the existence of restricted rotations in the complexes hence the protons could be subjected to different contributions from the ring currents from the pyrazole or pyridine groups on the NMR time scale. A similar spectrum has been reported for the related Cu complex, $[Cu\{(Me_2pz\text{-}CH_2)_2py\}(PPh_3)]ClO_4$, [7a] in which the $CH_2$ linker protons were observed as AB quartets at 4.75 and 5.25 ppm.

In complexes **3** and **4**, the $CH_2$ linker protons appeared as four distinct AB quartets with geminal coupling constants ranging from 15.4 to 19.2 Hz. This highlights the increased restricted rotation in **3** and **4** arising from the more sterically demanding ditertbutyl groups. The large peak separation of the signals ($\Delta\delta = 1.38$ ppm), however, is rather unusual. A smaller peak separation between the $CH_2$ linker protons ($\Delta\delta = 0.70$ ppm) of the related Ru complex of **L1**, $[Ru\{(\eta^6\text{-}C_6H_6)(Me_2pz\text{-}CH_2)_2py\}]PF_6$, [12] has been reported. Recently Cavell and co-workers reported even a smaller peak separation ($\Delta\delta = 0.07$ ppm) for geminal coupling of the bridging methylene protons of $[Pd(_{t\mathrm{Bu}}\hat{C}\hat{N}C)Me]BF_4$; a feature attributed to the slow inversion of the complex [13]. In contrast to our results, Cavell and co-workers found that in the chloro analogue, $[Pd(_{t\mathrm{Bu}}\hat{C}\hat{N}C)Cl]BF_4$, the methylene protons appear as a singlet at 5.69 ppm probably as a consequence of the lower *trans* effect of the $Cl^-$, which reduces the $Pd\text{–}N_{(py)}$ bond length and gives the ligand backbone greater ability to undergo unhindered rotation [13]. The $^1$H NMR spectra of **3** and **4** could be used to diagnose the bidentate bonding mode of compound **L2** in these complexes. For example in **3** one set of peaks at 1.41 and 1.75 ppm for tertbutyl protons and 5.92 ppm for the pyrazolyl ring proton were assigned to the bound pyrazolyl unit while peaks at 1.27 and 1.34 and 5.97 ppm were due to the 'dangling' pyrazolyl unit. This assignment is consistent with the solid state structure of **3** (*vide infra*). Similar spectra have been reported for compounds $[Ru\{(\eta^6\text{-}C_6H_6)(Me_2pz\text{-}CH_2)_2py\}]PF_6$ [12] and $[Pd\{(3,5\text{-}{}^tBu_2pz\text{-}CO)_2py\}Cl_2]$ [4].

### 3.2. Reactions of complexes *1–4* with $NaBAr_4$

In attempts to generate catalysts for the oligomerization or polymerization of ethylene, 8 mg of complexes **2** and **4** were reacted with either stoichiometric equivalent of $NaBAr_4$ or 1000-fold excess of modified methylaluminoxane (MMAO) in the presence of excess ethylene. We did not observe the formation of oligomers or polymers of ethylene as expected. In subsequent experiments performed on a preparative scale (Scheme 2), $^1$H NMR spectroscopic analyses suggested the formation of cationic species in which the ligands bind in a tridentate fashion upon chloride abstraction. These cationic species, $[Pd(_{\mathrm{Me}}\hat{N}\hat{N}N)Cl]^+$ (**5**), $[Pd(_{\mathrm{Me}}\hat{N}\hat{N}N)Me]^+$ (**6**) and $[Pd(_{t\mathrm{Bu}}\hat{N}\hat{N}N)Cl]^+$ (**7**), were isolated as $BAr_4^-$ salts and the structures of **5** and **6** (Figs. 2 and 3 respectively) confirmed the tridentate ligand coordination deduced from the spectroscopic data.

Recently we reported that $[Pd\{(3,5\text{-}Me_2pz\text{-}CO)_2py\}Cl_2]$ and $[Pd\{(3,5\text{-}{}^tBu_2pz\text{-}CO)_2py\}Cl_2]$ can be activated with methylaluminoxane (MAO) as co-catalyst to catalyze the polymerization of ethylene [4]. The inability of the cationic species generated from **2** and **4** to promote ethylene polymerization can be attributed to the strong coordination of the 'dangling' arm of the pyrazolyl unit in **2** and **4**, which blocks the vacant coordination site created upon chloride abstraction from the metal centre necessary for the coordination of the ethylene monomer. In the carbonyl linker analogues used to catalyze the polymerization of ethylene [4], it is likely that upon activation with MAO, similar tridentate cationic species are formed but under a high ethylene pressure, one of the coordinated pyrazolyl units dissociates from the Pd centre to allow the ethylene to coordinate and undergo subsequent insertion to form polyethylene (Scheme 1, route A). This behaviour is necessitated by the weaker binding ability of the pyrazolyl units in the carbonyl linker analogues. However, even when **6** and **7** were subjected to ethylene pressures up to 50 atm, there was no formation of polyethylene; an observation which highlights the strength of the $Pd\text{–}N_{(pz)}$ bonds in **6** and **7** relative to the binding affinity of the ethylene monomer.

### 3.3. Oligomerization and polymerization of phenylacetylene

The binding affinity of the monomer is important since in experiments using phenylacetylene instead of ethylene, we did observe the formation of oligomers and polymers of phenylacetylene (Table 1). The active catalysts were generated by reacting complexes **1–4** with AgOTf as halide abstractor in a mixture of $CH_2Cl_2$ and MeCN (3:1). The ability of catalysts generated from **1** to **4** to oligomerize and polymerize phenylacetylene therefore highlights the significance of the reactivity and the binding affinity of the incoming monomer in displacing or competing with one of the $Pd\text{–}N_{(pz)}$ bonds prior to coordination to the metal centre (Scheme 3, route A). However, the low percentage conversions observed for catalysts **1–4** (36–55%) compared to 90% conversion [10] obtained for the carbonyl linker and bis(pyrazole)palladium(II) complexes under similar conditions suggests the possibility of a competing deactivation pathway. This could arise from the formation of the inactive cationic tridentate species (Scheme 3, route B) which blocks monomer coordination. This argument

Table 1
Phenylacetylene oligomerization and polymerization data[a]

| Entry | Catalyst | % Conversion[b] | $M_w$[c] | $M_n$[c] | $M_w/M_n$[c] | % *cis*[d] |
|---|---|---|---|---|---|---|
| 1 | **1** | 51 | 2552 | 1575 | 1.62 | 44 |
| 2 | **2** | 47 | 3444 | 1893 | 1.82 | 80 |
| 3 | **3** | 36 | 2303 | 1466 | 1.57 | 56 |
| 4 | **4** | 38 | 2062 | 1350 | 1.52 | 74 |
| 5 | **1**[e] | 35 | 2716 | 1697 | 1.72 | |
| 6 | **1**[f] | 55 | 2230 (620) | 1523 (619) | 1.48 (1.00) | |
| 7 | **2**[g] | 47 | 3613 (684) | 2187 (678) | 1.65 (1.01) | |
| 8 | **2**[h] | 12 | 860 | 797 | 1.01 | |

[a] Conditions: Time = 60 min unless stated otherwise; amount of monomer = 0.64 mL; solvent: $CH_2Cl_2$:MeCN (40 mL); 3:1, temp = 25 °C; [Pd] = $1.0 \times 10^{-3}$ mol; phenylacetyelene:[Pd] = 50:1.
[b] Determined by the total mass of the crude product as a percentage of monomer used.
[c] Determined by room temperature GPC using polystyrene standards.
[d] Determined by $^1$H NMR analysis: *cis* % = $[A_{5.82}/(A_{total}/6)] \times 100$ or *cis* % $A_{5.82} \times 10^4/A_{total} \cdot 16.66$ ($A_{5.82}$ is the integrated peak area of the vinyl proton in the *cis* isomer and $A_{total}$ is the total integrated peak area of the polymer spectrum).
[e] Time = 30 min.
[f] Time = 120 min.
[g] Crude product (mixture of oligomer and polymer).
[h] Oligomer fraction.

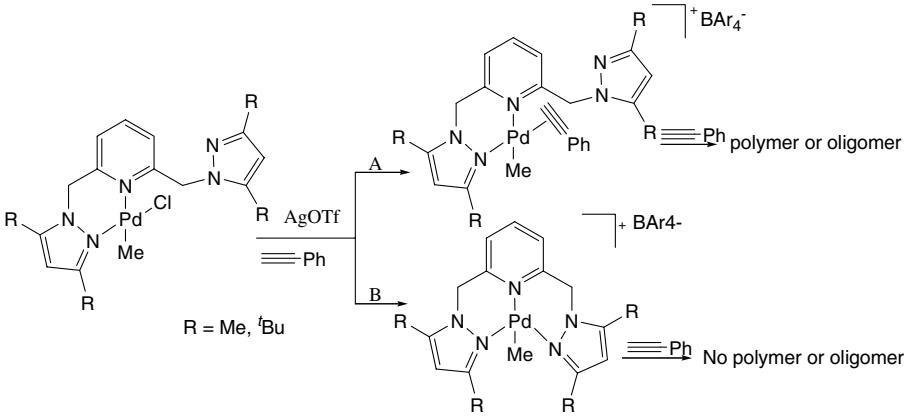


Scheme 3.

also supports the slow initiation process observed with systems **1**–**4** as opposed to rapid initiation observed with simple pyrazole and carbonyl linker pyrazolyl palladium complexes [14].

Generally catalysts **1** and **2** bearing methyl substituents on the pyrazolyl ligand showed higher activity than the tertbutyl analogues **3** and **4** (Table 1, entries 1–4). It is likely that the bulkier tertbutyl group hinders monomer coordination resulting in low product yields. We have examined the structurally characterized complexes **3**, **5**, **6**, **11** and **12** from the point of view of the ligand solid angles expressed in percentage of the metal coordination sphere shielded by each ligand. Such an approach provides a quantitative measure of the steric bulk of the ligands [15]. The tridentate ligands in **5**, **6** and **11** shield on average 59.6(10)% of the palladium coordination sphere. The $\kappa^3$-($_{t\text{Bu}}\hat{\text{N}}\hat{\text{N}}\hat{\text{N}}$) ligand in **12** shields an enormous 70.1% of the central metal, and the difference of over 10% from its methyl analogue is very significant in terms of dynamic behaviour. As a reference, even ca. 1% changes in the value of a ligand solid angle can affect the ligand's coordination mode [16]. However, it is interesting to note the size of the $\kappa^2$-($_{t\text{Bu}}\hat{\text{N}}\hat{\text{N}}\text{N}$) ligand in **3**; the shielding percentage of this ligand is only 51.0%, and thus the flexibility of ($_{t\text{Bu}}\hat{\text{N}}\hat{\text{N}}\text{N}$) can play a major role in the kinetics of the system. Time dependent polymerization experiments with catalyst **1** (Table 1, entries 1, 5 and 6) showed little variation in the percent conversion of monomer after 60 min. This is a typical feature involving catalyst decomposition with time [17] and in our case would suggest active catalysts forming tridentate species via route B in Scheme 3.

The stereochemistry of the polymers was determined by $^1$H NMR spectroscopy. A typical $^1$H NMR spectrum of polymers obtained showed a sharp singlet at 5.85 ppm for the vinylic protons, and broad singlets at 6.65 and 6.91 ppm corresponding to the phenyl *ortho* and *meta* protons respectively. From the $^1$H NMR data, it is evident that all the polymers were a mixture of *cis-transoidal* and

*trans-cisoidal* [18] with the percentage *cis* content ranging from 44 to 80 (Table 1, entries 1–4). The *cis* and *trans* content of the polyphenylacetylene formed were established by the NMR method reported by Perec et al. [18a] and the formula to calculate the *cis* and *trans* content of the polymer is included as a footnote in Table 1. However, there was no clear dependence of the polymer stereochemistry with respect to catalyst structure.

GPC analysis showed the presence of both oligomers ($M_w = 620$–$860$) and low molecular weight polymers ($M_w = 2062$–$3444$) (Table 1, entries 1–4, 7 and 9). For example analysis of the crude products from catalysts **2** (Table 1, entry 7) gave a bimodal distribution GPC trace corresponding to oligomers of average $M_w$ of 684 and polymers of average $M_w$ of 3613. Upon purification of this product, the oligomers (methanol soluble fraction) and polymers (methanol insoluble) gave average $M_w$ of 860 and 3444 respectively.

Table 2
Selected $^1$H NMR signals and half lives ($t_{1/2}$) of the cationic complexes **5**–**10** in $CDCl_3$

| Compound | $^1$H NMR ($CDCl_3$, ppm) | | | | $t_{1/2}$ (days) |
|---|---|---|---|---|---|
| | $CH_2$ | 4H-pz | $_R$pz (R = Me or $^t$Bu) | 4H-py | |
| **5** | 5.25, 5.95 | 5.99 | 2.35, 2.57 | 7.27 | >30 |
| **6** | 5.14, 5.70 | 5.95 | 2.30, 2.35 | 7.55 | >30 |
| **7** | 5.74, 6.31 | 6.07 | 1.41, 1.66 | 7.40 | >30 |
| **8** | 5.68, 6.21 | 6.08 | 1.41, 1.52 | 7.50 | >30 |
| **9** | | 6.38 | 2.57, 2.67 | 8.04 | 14 |
| **10** | | 6.57 | 1.17, 1.76 | 8.01 | 2 |

### 3.4. Stability of cationic and neutral species of *1–4*

Following the attempts to establish the ability of **2** and **4** to produce active catalysts for ethylene polymerization as described above, we investigated the stability of the cationic species with $CH_2$ and CO linkers using complexes **1**–**4**, [Pd{(3,5-$Me_2$pz-CO)$_2$py}$Cl_2$] and [Pd{(3,5-$^t$Bu$_2$pz-CO)$_2$py}$Cl_2$]. In a typical experiment, **1** (6 mg, 0.012 mmol) and $NaBAr_4$ (12 mg, 0.012 mmol) were placed in a J-Young NMR tube and about 0.4 mL $CDCl_3$ added and the reaction followed by $^1$H NMR spectroscopy. In all cases the cationic species of **1**–**4** were formed within 10 min but reactions of the CO linker analogues took up to 4 h to go to completion. The stability of the cationic species [Pd($_{Me}$ÑÑN)Cl]$^+$ (**5**), [Pd($_{Me}$ÑÑN)Me]$^+$ (**6**), [Pd($_{tBu}$ÑÑN)Cl]$^+$ (**7**), [Pd($_{tBu}$ÑÑN)Me]$^+$ (**8**), [Pd{(3,5-$Me_2$pz-CO)$_2$py}Cl]$^+$ (**9**) and [Pd{(3,5-$^t$Bu$_2$pz-CO)$_2$py}Cl]$^+$ (**10**) also varied. By using the proton peaks of the $BAr_4^-$ counter ion in these salts as internal standard, we established that species **5**–**8** were stable for 30 days without any signs of decomposition while the carbonyl linker counterparts, **9** and **10**, had $t_{1/2}$ of 14 and 2 days respectively (Table 2). The low stability of **9** and **10** may arise from the effect of the carbonyl group in reducing the donor ability of the pyrazolyl nitrogen atoms in **9** and **10** compared to the cations with methylene linkers, **5**–**8**. The stability of the cationic species **5**–**8** might explain why reactions of **1**–**4** with either MMAO or $NaBAr_4$ did not result in the production of active ethylene polymerization catalysts.

Another interesting observation made during attempts to grow crystals of complexes **1**–**4** is that the species that crystallized depended on the procedure used. Attempts to

Table 3
Crystal data and structure refinement parameters for compounds **3**, **5**, **6**, **11** and **12**

| Parameter | **3** | **5** | **6** | **11** | **12** |
|---|---|---|---|---|---|
| Formula | $C_{31}H_{47}Cl_8N_5Pd$ | $C_{50}H_{35}BCl_3F_{24}N_5Pd$ | $C_{50}H_{36}BF_{24}N_5Pd$ | $C_{38}H_{46}Cl_{20}N_{10}Pd_4$ | $C_{64}H_{102}Cl_{20}N_{10}Pd_4$ |
| Fw | 879.74 | 1385.39 | 1280.05 | 1777.45 | 2146.16 |
| Temperature (K) | 100(2) | 100(2) | 100(2) | 100(2) | 100(2) |
| Wavelength (Å) | 0.71073 | 0.71073 | 0.71073 | 0.71073 | 0.71073 |
| Cryst system | triclinic | monoclinic | monoclinic | triclinic | triclinic |
| Space group | $P\bar{1}$ | $P2_1/n$ | $P2_1/n$ | $P\bar{1}$ | $P\bar{1}$ |
| *A* (Å) | 10.7180(15) | 15.498(2) | 10.8623(16) | 9.6999(17) | 10.0902(10) |
| *B* (Å) | 12.6687(19) | 9.2217(12) | 17.848(3) | 9.7901(17) | 14.1549(14) |
| *C* (Å) | 15.490(2) | 38.010(5) | 26.862(4) | 17.018(3) | 15.7395(15) |
| $\alpha$ (°) | 87.557(3) | 90 | 90 | 87.410(3) | 88.201(2) |
| $\beta$ (°) | 70.102(2) | 100.563(2) | 96.444(2) | 89.354(3) | 85.368(2) |
| $\gamma$ (°) | 81.527(3) | 90 | 90 | 64.335(3) | 77.909(2) |
| Volume (Å$^3$) | 1956.05(4) | 5340.5(12) | 5174.7(13) | 1455.1(4) | 2190.7(4) |
| *Z* | 2 | 4 | 4 | 1 | 1 |
| $D_{calc.}$ (Mg/m$^3$) | 1.494 | 1.723 | 1.643 | 2.028 | 1.627 |
| Absorption coefficient (mm$^{-1}$) | 1.050 | 0.624 | 0.487 | 2.176 | 1.461 |
| *F*(000) | 900 | 2752 | 2552 | 868 | 1080 |
| Final *R* indices ($R_1$) | 0.0509 | 0.0640 | 0.0409 | 0.0626 | 0.0355 |
| Reflections collected | 9611 | 41 777 | 42 250 | 16 921 | 13 905 |
| Completeness to theta (%) | 95.2 | 99.6 | 99.8 | 92.8 | 89.3 |
| Goodness-of-fit on $F^2$ | 1.030 | 1.067 | 1.097 | 0.977 | 1.036 |
| Largest difference peak and hole (e Å$^{-3}$) | 1.220 and −0.600 | 3.243 and −1.802 | 1.353 and −1.309 | 1.275 and −1.660 | 0.835 and −0.636 |

grow crystals of **1** and **3** directly from the mother liquor (reaction mixture) gave crystals of tridentately bound cationic species with $[Pd_2Cl_6]^{2-}$ as counter ion (**11** and **12**) within 7 days. On the other hand, when **3** was precipitated out initially from the reaction mixture and subsequently re-dissolved in $CH_2Cl_2$, crystals of **3** were obtained. Crystals of **3** were dissolved in $CDCl_3$ and monitored for 21 days by $^1H$ NMR but showed no signs of forming the cationic species **12**. It is not clear what causes the formation of **11** and **12** from the reaction mixture which does not occur when **1** and **3** are first isolated and re-dissolved in $CH_2Cl_2$. However, both **11** and **12** crystallized with solvent molecules and rapidly lost solvent when crystals were removed from the mother liquor and became insoluble. It was therefore difficult to further characterize these materials.

### 3.5. Molecular structure determination by single crystal X-ray crystallography

Single crystals suitable for X-ray analysis of complexes **3** and **5** were grown by slow evaporation of the dichloromethane solvent at room temperature while crystals of **6** were grown by slow diffusion of hexane into dichloromethane at −4 °C. In other attempts to obtain crystals of **1** and **3**, cationic tridentate palladium complexes $2[(_{Me}\hat{N}\hat{N}\hat{N})PdCl]^+$ (**11**) and $2[(_{tBu}\hat{N}\hat{N}\hat{N})PdCl]^+$ (**12**) with $[Pd_2Cl_6]^{2-}$ counter ions were obtained as described earlier.

Crystallographic data for **3**, **5**, **6**, **11** and **12** are presented in Table 3, while selected bond lengths and angles are given in Table 4. Solid state structures of **3**, **5**, **6**, **11** and **12** are shown in Figs. 1–5 respectively. The five palladium complexes contain the central metal in a slightly distorted

Table 4
Selected bond lengths (Å) and bond angles (°) for **3**, **5**, **6**, **11** and **12**

| | **3** X = Cl(2) | **5** X = Cl(1) | **6** X = C(1) | **11** X = Cl(1) | **12** X = Cl(1) |
|---|---|---|---|---|---|
| *Bond lengths* | | | | | |
| Pd(1)–N(1) | 2.026(3) | 2.007(4) | 2.028(2) | 2.011(5) | 2.029(2) |
| Pd(1)–N(3) | 2.042(3) | 2.031(4) | 2.128(2) | 2.010(5) | 1.9925(19) |
| Pd(1)–N(5) | | 2.023(4) | 2.043(2) | 2.012(5) | 2.028(2) |
| Pd(1)–X | 2.3125(5) | 2.2803(13) | 2.029(3) | 2.2838(18) | 2.2872(6) |
| N(1)–N(2) | 1.371(4) | 1.366(6) | 1.369(3) | 1.381(7) | 1.381(3) |
| N(4)–N(5) | 1.371(4) | 1.367(6) | 1.370(3) | 1.356(7) | 1.378(3) |
| *Bond angles* | | | | | |
| N(1)–Pd(1)–N(3) | 84.00(13) | 87.39(17) | 86.07(9) | 88.81(2) | 84.87(10) |
| N(3)–Pd(1)–X | 173.92(10) | 177.63(12) | 175.95(11) | 175.1(1) | 178.69(6) |
| N(1)–Pd(1)–X | 94.36(10) | 91.07(12) | 93.73(15) | 92.13(11) | 94.59(9) |
| N(1)–Pd(1)–N(5) | | 175.85(17) | 172.90(9) | 175.1(2) | 170.77(8) |
| N(3)–Pd(1)–N(5) | | 88.57(17) | 88.03(9) | 86.9(2) | 85.94(8) |

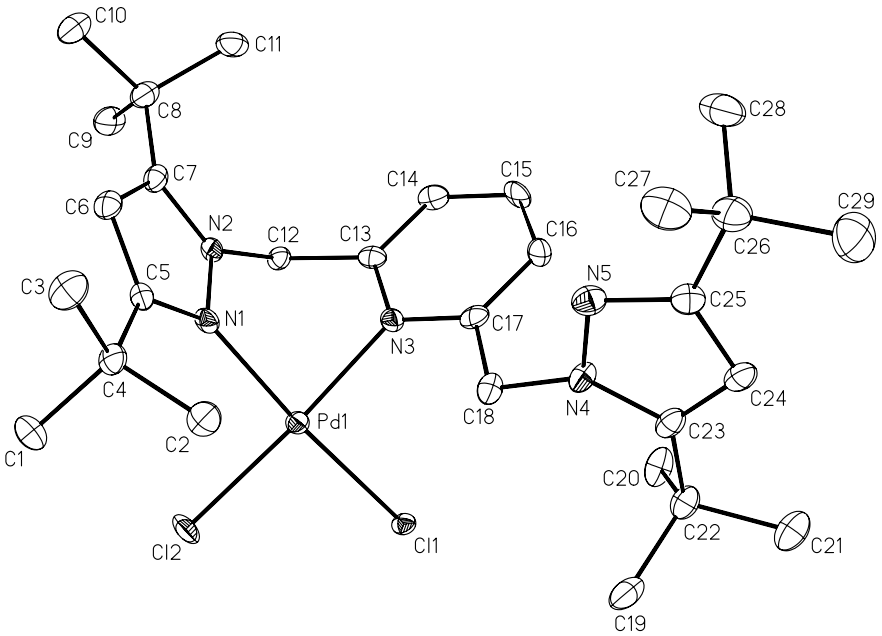


Fig. 1. Molecular structure of complex **3** shown with 50% probability ellipsoids. The hydrogen atoms are omitted for clarity.

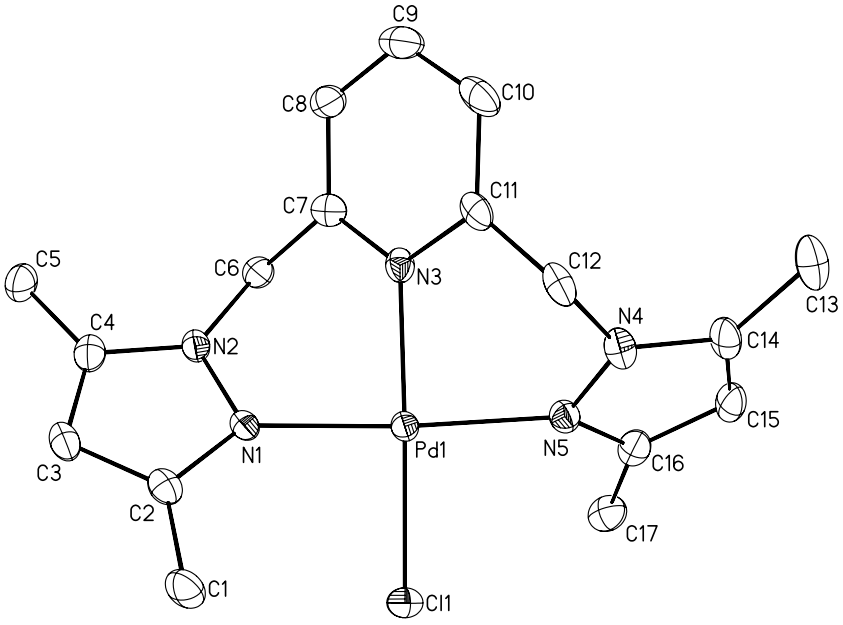


Fig. 2. Molecular structure of cation of **5** shown with 50% probability ellipsoids. The boron counter ion and hydrogen atoms are omitted for clarity.

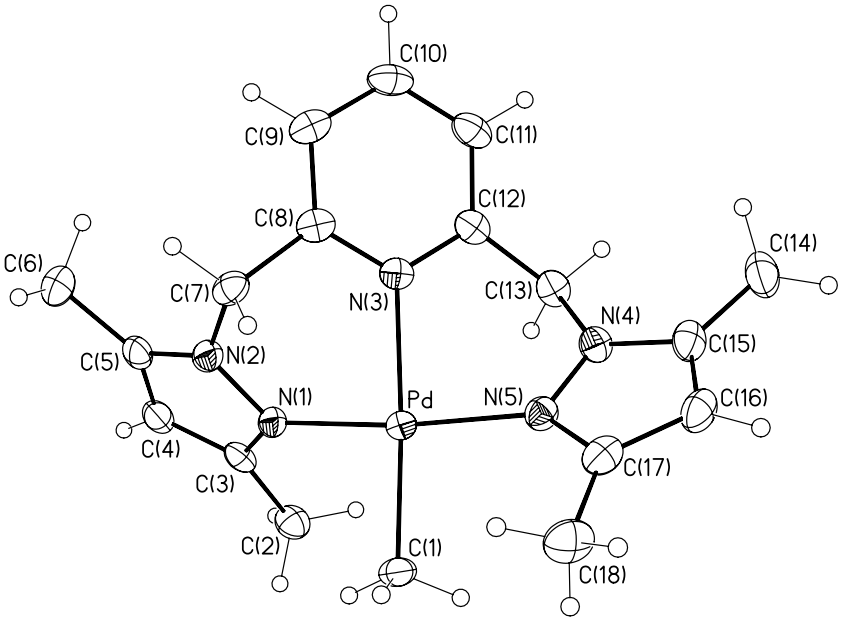


Fig. 3. Molecular structure of cation of **6** shown with 50% probability ellipsoids. The boron counter ion is omitted for clarity.

square planar geometry. In the structure of **3** (Fig. 1) the nitrogen atom, N5, of the free pyrazolyl unit is directed away from the palladium metal. It is therefore evident that the rotation about the $CH_2$ linker in the $\kappa^2$-2,6-{(3,5-$^t$Bu$_2$pzCH$_2$)$_2$py} ligand yields a $\kappa^3$-2,6-{(3,5-$^t$Bu$_2$pzCH$_2$)$_2$py} ligand in the cationic species **12** (Fig. 5). The $[Pd_2Cl_6]^{2-}$ in the structures of **11** and **12** occupies a crystallographic inversion centre with the two cationic palladium complexes residing on each side of the anion. The spatial arrangement of the cationic palladium moieties in **11** and **12** is such that the Pd–Cl bonds of the cationic complexes are facing away from the central $[Pd_2Cl_6]^{2-}$ unit.

The average bond lengths of the Pd–$N_{(pz)}$ of 2.026(3), 2.015(11), 2.026(11), 2.012(5) and 2.029(2) Å of complexes **3**, **5**, **6**, **11** and **12** respectively are all slightly shorter than the average Pd–N(pz) bond length of 2.06(9) Å obtained by averaging 607 bonds in 229 relevant complexes reported to the Cambridge Structural Database (CSD) [19] but the difference is not statistically significant because of the high uncertainties for the average Pd–$N_{(pz)}$ bond length of 2.06(9) Å.

The average Pd–N(pz) distance of 2.015(11) Å in **5** is somewhat shorter than that in **6** (2.036(11) Å), however the difference is not statistically significant. On the other

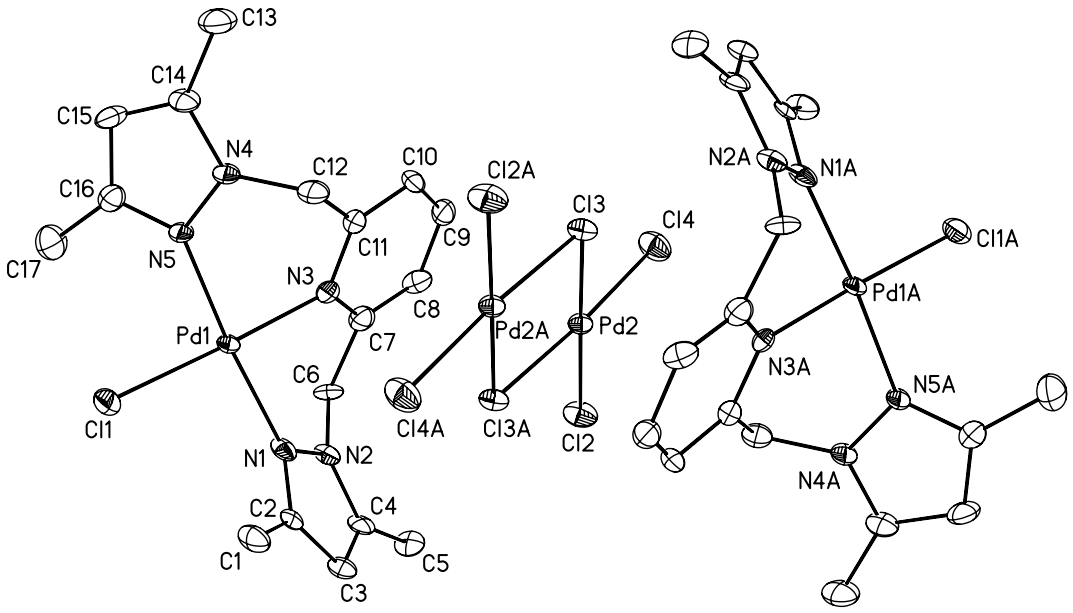


Fig. 4. Molecular structure of compound **11** shown with 50% probability ellipsoids. The hydrogen atoms are omitted for clarity.

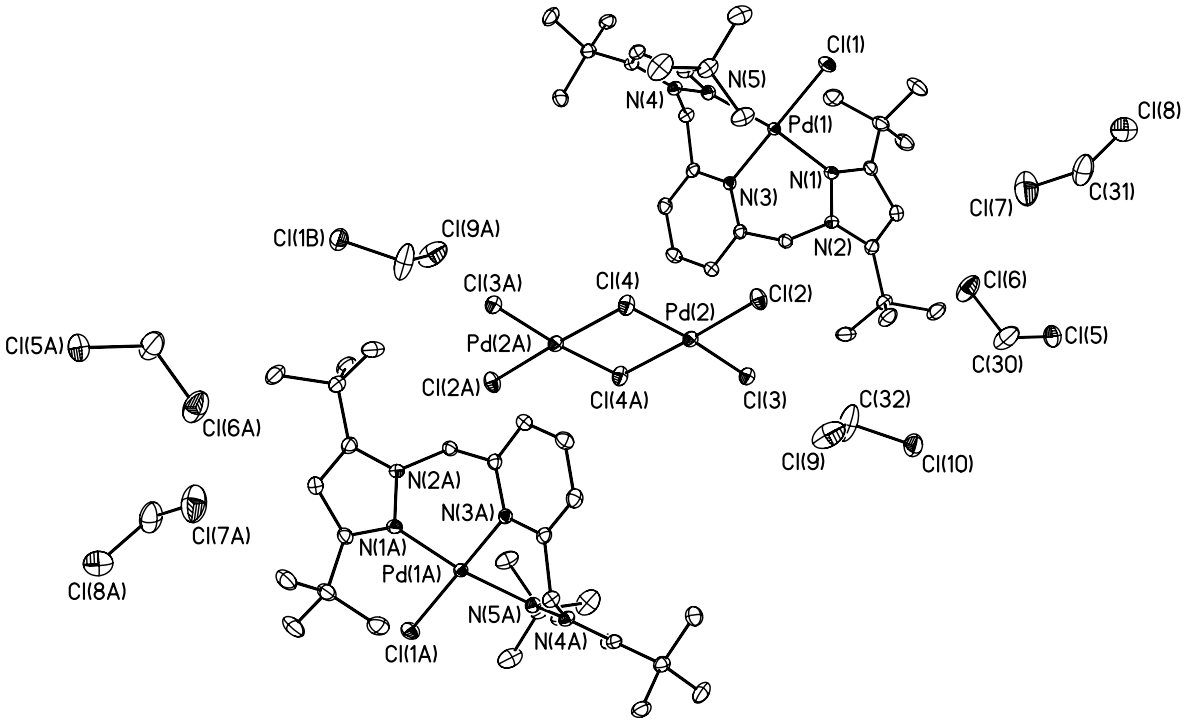


Fig. 5. Solid state structure of solvated complex **12** shown with 50% probability ellipsoids. The hydrogen atoms are omitted for clarity.

hand, the Pd–N(py) distance in **6** is substantially longer than those in **5**, **11** and **12**, and that is attributed to the high *trans* influence of the methyl group as compared to the chloro ligand. A shorter Pd–N(py) bond length 2.128(2) Å for **6** and 2.031(4) Å for **5**. A shorter Pd–$N_{(py)}$ bond length of 2.036(3) Å has been recently reported for the chloro complex, [Pd(ĈN̂C)Cl]$BF_4$ compared to 2.116(3) Å of the methyl analogue, [Pd(ĈN̂C)Me]$BF_4$ [20]. The average bond length of Pd–$N_{(py)}$ of 2.028(2) Å and Pd–C of 2.044(1) Å of **6** are significantly shorter than those reported for the carbene methylene bridged cationic Pd complex [Pd(ĈN̂C)Me]$BF_4$ of 2.0154(9) and 2.044(1) Å respectively [20]. The Pd–Cl bond distances of 2.3125(5) Å (**3**), 2.2803(13) Å (**5**), 2.2838(18) Å (**11**) and 2.2872(6) Å (**12**) in the mononuclear complexes agree well with the average bond distances of 2.33(5) Å determined by averaging 2055 Pd–Cl bonds in 1268 relevant complexes reported to the CSD [19]. Interestingly, the average Pd–$N_{(pz)}$ bond distances of 2.026(3) Å (**3**) and 2.029(2) Å (**12**) and Pd–Cl bond distances of 2.3125(5) Å (**3**) and

2.2872(6) Å (**12**) are statistically similar even though the Pd metal in **12** is more electrophilic and is expected to have shorter bond distances. Surprisingly, the longer $Pd–N_{(pz)}$ distance of 2.012(5) Å is observed for **11** than for **12** (2.028(2) Å) that contains a bulkier tridentate ligand.

## 4. Conclusions

The potentially tridentate bis(pyrazolylmethyl)pyridine compounds form monometallic palladium complexes with one uncoordinated pyrazolyl unit when complexed with either $[PdCl_2(NCMe)_2]$ or [Pd(COD)MeCl]. Coordination of the dangling pyrazolyl unit upon chloride abstraction in an attempt to generate catalysts for ethylene oligomerization or polymerization results in the formation of inactive cationic tridentate species. The same palladium complexes however, do form catalysts that catalyze the oligomerization and polymerization of the more reactive phenylacetylene producing a mixture of oligomers and low molecular weight polyphenylacetylene. Competitive coordination of phenylacetylene and the second pyrazolyl unit to the Pd metal centre appears to control the catalysis process. The polydentate ligands were also characterized with the use of the ligand solid angles.

## Acknowledgement

Funding for this project was provided by National Research Foundation, Department of Science and Technology, Centre of Excellence in Catalysis (NRF-DST, c*change) South Africa.

## Appendix A. Supplementary material

CCDC 605039, 606395, 604750, 604751, and 604749 contains the supplementary crystallographic data for **3**, **5**, **6**, **11**, and **12**. These data can be obtained free of charge via http://www.ccdc.cam.ac.uk/conts/retrieving.html, or from the Cambridge Crystallographic Data Centre, 12 Union Road, Cambridge CB2 1EZ, UK; fax: (+44) 1223-336-033; or e-mail: deposit@ccdc.cam.ac.uk. Supplementary data associated with this article can be found, in the online version, at doi:10.1016/j.poly.2006.09.007.

## References

[1] (a) S. Ittel, M. Brookhart, L.K. Johnson, Chem. Rev. 100 (2000) 1169;
(b) S. Mecking, Coord. Chem. Rev. 203 (2000) 325;
(c) V.C. Gibson, S.K. Spitzmesser, Chem. Rev. 103 (2003) 283;
(d) C. Bianchini, G. Giambastiani, I.G. Rios, G. Mantovani, A. Meli, A.M. Segarra, Coord. Chem. Rev. 250 (2006) 1391.
[2] (a) C.M. Killian, L.K. Johnson, M. Brookhart, Organometallics 16 (1997) 2005;
(b) S.A. Srejda, L.K. Johnson, M. Brookhart, J. Am. Chem. Soc. 121 (1999) 10634.
[3] (a) L.K. Johnson, C.M. Killian, M. Brookhart, J. Am. Chem. Soc. 117 (1995) 6414;
(b) S. Mecking, L.K. Johnson, M. Brookhart, J. Am. Chem. Soc. 118 (1996) 267;
(c) P.K. Byers, A.J. Canty, B.W. Skelton, A.H. White, J. Organomet. Chem. 393 (1990) 299.
[4] M.S. Mohlala, I.A. Guzei, J. Darkwa, S.F. Mapolie, J. Mol. Catal. A: Chem. 241 (2005) 93.
[5] (a) I.A. Guzei, K. Li, G.A. Bikzhanova, J. Darkwa, S.F. Mapolie, Dalton Trans. 715 (2003);
(b) K. Li, I.A. Guzei, J. Darkwa, S.F. Mapolie, J. Organomet. Chem. 660 (2002) 108.
[6] (a) A.A. Watson, D.A. House, P.J. Steel, Inorg. Chim. Acta 130 (1987) 167;
(b) D.A. House, P.J. Steel, A.A. Watson, Aus. J. Chem. 48 (1995) 1549.
[7] (a) S. Mahapatra, R.N. Mukherjee, J. Chem. Soc., Dalton Trans. (1991) 2911;
(b) N. Gupta, S. Mukherjee, S. Mahapatra, M. Ray, R.N. Mukherjee, Inorg. Chem. 31 (1992) 139;
(c) A.R. Karam, E.L. Catari, F.L. Linares, G. Agrifoglio, C.L. Albano, A.D. Barrios, T.E. Lehmann, S.V. Pekerar, L.A. Albornoz, R. Atencio, T. Gonzalez, H.B. Ortega, P. Joskowics, Appl. Catal. A: Gen. 280 (2005) 165.
[8] J. Elguero, E.J.R. Jacquier, Bull. Soc. Chim. Fr. 2 (1968) 707.
[9] D. Drew, J.R. Doyle, Inorg. Synth. 13 (1972) 47.
[10] E. Rule, I.M. Han, C.J. Elsevier, K. Vrieze, P.W.N.M. Van Leeuwen, C.F. Roobeek, M.C. Zoutberg, Y.F. Wand, C.H. Stam, Inorg. Chim. Acta 169 (1990) 5.
[11] Bruker-AXS SADABS V.2.05, SAINT V.6.22, SHELXTL V.6.10 & SMART 5.622 Software Reference Manuals. Bruker-AXS, Madison, WI, USA, 2000–2004.
[12] Z. Shirin, R. Mukherjee, J.F. Richardson, R.M. Buchanan, J. Chem. Soc., Dalton Trans. (1994) 465.
[13] D.J. Nielsen, K.J. Cavell, B.W. Skelton, A.H. White, Inorg. Chim. Acta 359 (2006) 1855.
[14] K. Li, M.S. Mohlala, T.V. Segapelo, P.M. Shumbula, I.A. Guzei, J. Darkwa, unpublished results.
[15] I.A. Guzei, M. Wendt, Dalton Trans. (2006) 3991.
[16] G.K. Fukin, I.A. Guzei, E.V. Baranov, J. Coord. Chem., in press.
[17] Y. Chen, R. Chen, C. Qian, X. Dong, J. Sun, Organometallics 22 (2003) 4312.
[18] (a) C.I. Simionescu, V. Percec, S.J. Dumetrescu, Polym. Chem. Ed. 15 (1977) 2497;
(b) A.Forlani, S. Liccocia, M.V. Russo, J. Polym. Sci. A: Polym. Chem. 24 (1986) 991.
[19] F.H. Allen, Acta Crystallogr., Sect. B 58 (2002) 380.
[20] D.J. Nielsen, K.J. Cavell, B.W. Skelton, A.H. White, Inorg. Chim. Acta 327 (2002) 116.